



Intramolecular recombination enables the formation of hepatitis B virus (HBV) cccDNA in mice after HBV genome transfer using recombinant AAV vectors

Chunkyu Ko^{a,c}, Jinpeng Su^a, Julia Festag^a, Romina Bester^a, Anna D. Kosinska^{a,b},
Ulrike Protzer^{a,b,*}

^a Institute of Virology, Technical University of Munich/Helmholtz Zentrum München, Munich, Germany

^b German Center for Infection Research (DZIF), Munich partner site, Munich, Germany

^c Infectious Diseases Therapeutic Research Center, Therapeutics & Biotechnology Division, Korea Research Institute of Chemical Technology, Daejeon, Republic of Korea

ARTICLE INFO

Keywords:

Hepatitis B virus
cccDNA
Adeno-associated virus
Recombination
Mouse liver

ABSTRACT

The mouse is not a natural host of hepatitis B virus (HBV) infection and - despite engraftment of hepatocytes with the HBV receptor - does not support formation of HBV covalently closed circular (ccc) DNA serving as a template for viral transcription and permitting persistent infection. In a recent study, cccDNA formation in mouse hepatocytes has been described following an HBV genome delivery by a recombinant, adeno-associated virus vector (rAAV) (Lucifora et al., 2017). The integrity of HBV cccDNA, its origin and functionality, however, remained open. In this study, we investigated the identity, origin, and functionality of cccDNA established in mice infected with rAAV carrying 1.3-fold overlength HBV genomes. We show that replication of HBV genotypes A, B, C and D can be initiated in mouse livers, and that cccDNA derived from all genotypes is detected. Restriction enzyme and exonuclease digestion as well as sequencing analysis of cccDNA amplicons revealed authentic HBV cccDNA without any detectable alteration compared to cccDNA established after HBV infection of human liver cells. Mouse livers transduced with a core protein-deficient HBV using rAAV still supported cccDNA formation demonstrating that the genesis of cccDNA was independent of HBV replication. When mice were infected with an rAAV-HBV1.3 carrying premature stop codons in the 5' but not in the 3' core protein open reading frame, the stop codon was partially replaced by the wild-type sequence. This strongly indicated that intramolecular recombination, based on >900 identical base pairs residing at the both ends of the HBV1.3 transgene was the origin of cccDNA formation. Accordingly, we observed a constant loss of cccDNA molecules from mouse livers over time, while HBeAg levels increased over the first two weeks after rAAV-HBV1.3 infection and remained constant thereafter, suggesting a minor contribution of the cccDNA molecules formed to viral transcription and protein expression. In summary, our results provide strong evidence that intramolecular recombination of an overlength, linear HBV genome, but not HBV genome recycling, enables cccDNA formation in rAAV-HBV mouse models.

1. Introduction

Hepatitis B virus (HBV) infection is a public health problem with more than 250 million chronically infected individuals worldwide (WHO, 2019). Chronic hepatitis B is still the leading cause of liver-related morbidity and mortality and accounts for an 887,000

HBV-related deaths per year.

HBV is an enveloped, DNA virus that belongs to the *Hepadnavirus* family (Seeger and Mason, 2015). HBV contains a partially double-stranded (ds) relaxed circular (rc) DNA genome of approximately 3.2 kilobases (kb) in its icosahedral capsid. When HBV has entered its host cell, the hepatocyte, the capsid delivers the viral rcDNA

Abbreviations: HBV, hepatitis B virus; rcDNA, relaxed circular DNA; rAAV, recombinant adeno-associated virus; NTCP, sodium taurocholate cotransporting polypeptide; cccDNA, covalently closed circular DNA; pgRNA, pregenomic RNA; dsDNA, double-stranded linear DNA; WT, wild-type; MOL, multiplicity of infection; HBeAg, HBV e antigen.

* Corresponding author. Ulrike Protzer Institute of Virology, Technical University of Munich/Helmholtz Zentrum München, Trogerstrasse 30, 81675, Munich, Germany.

E-mail address: protzer@tum.de (U. Protzer).

<https://doi.org/10.1016/j.antiviral.2021.105140>

Received 6 January 2021; Received in revised form 9 July 2021; Accepted 12 July 2021

Available online 17 July 2021

0166-3542/© 2021 Elsevier B.V. All rights reserved.

genome to the nucleus where it is converted to covalently closed circular (ccc) DNA by host DNA repair enzymes (Kitamura et al., 2018; Koniger et al., 2014; Long et al., 2017; Qi et al., 2016; Sheraz et al., 2019; Wei and Ploss, 2020). The nuclear cccDNA persists in the nucleus as a mini-chromosome and serves as transcription template for all viral RNAs, including a pregenomic RNA (pgRNA) (Nassal, 2015).

Viral genome replication begins with the recognition of a stem-loop structure located near the 5' end of the viral pgRNA by the HBV polymerase (Bartenschlager et al., 1990; Tavis et al., 1994). This complex is then incorporated into a newly forming capsid inside which viral reverse transcription takes place to generate a new rcDNA genome. rcDNA-containing, mature capsids are enveloped by a lipid shell containing the three viral envelope proteins (L-HBs, M-HBs, and S-HBs) and released as progeny viruses. Alternatively, the mature capsids can deliver rcDNA into the nucleus to maintain or amplify the cccDNA pool, termed intracellular genome recycling or intracellular cccDNA amplification (Ko et al., 2018).

HBV has a narrow host range for humans and humanoids apes and a strict liver tropism efficiently targeting hepatocytes. Murine hepatocytes are not permissive for HBV infection due to host restrictions at two distinct early steps in the HBV life cycle. HBV exploits the human sodium taurocholate cotransporting polypeptide (hNTCP), a hepatic bile acid transporter, as an entry receptor (Ni et al., 2014; Yan et al., 2012). HBV particles are capable of binding to the mouse homolog of hNTCP (mNTCP), but mNTCP does not support HBV infection due to sequence differences at amino acid residues 84–87 (Yan et al., 2013). Cell lines and transgenic mice expressing hNTCP gain susceptibility for hepatitis delta virus, an HBV satellite virus coated with HBV envelope proteins that shares the same receptor for cellular entry but only needs to reach the cytoplasm for replication (He et al., 2015; Lempp et al., 2016b; Li et al., 2014; Yan et al., 2013). Reconstitution of mouse cell lines with hNTCP, however, still did not render them permissive for HBV pointing at a second restriction downstream of viral entry. On the other hand, mouse hepatocytes allow HBV gene expression following nuclear delivery of a replication-competent HBV genome e.g. bypassing the true entry process and introducing an artificial HBV transcriptional template (Lempp et al., 2016a; Li et al., 2014; Sprinzl et al., 2001). This highlights additional restriction for HBV infection in mouse cells that occurs after viral entry but prior to transcription of HBV-DNA in the nucleus – most likely during nuclear delivery of HBV genomes.

Given that mouse hepatocytes support HBV transcription and subsequent steps leading to the production of infectious virions (Guidotti et al., 1995; Sprinzl et al., 2001), several mouse models have been developed (Allweiss and Dandri, 2016; Hu et al., 2019; Protzer, 2017). Among those, adeno-associated virus (AAV)-mediated HBV genome delivery into mouse hepatocytes has been shown to best support sustained HBV replication and antigen expression (>1 year), rendering this model suitable for studying the mechanism of HBV-specific tolerance and evaluating novel antivirals or immunotherapeutic strategies to treat chronic HBV infection (Dion et al., 2013; Michler et al., 2020; Yang et al., 2014).

AAV belongs to the *parvoviridae* family and contains a single-stranded (ss) DNA genome of approximately 4.7 kb in a non-enveloped, icosahedral capsid (Hastie and Samulski, 2015). AAV is a naturally replication-defective virus, which requires co-infection with a helper virus, such as adenovirus or herpesviruses for a productive infection. The AAV genome only encodes two genes (*rep* and *cap*) flanked by two T-shaped inverted terminal repeats (ITRs) that can be completely replaced with a gene of interest with the size limit of ~4.9 kb to produce recombinant AAV (rAAV) (Dong et al., 1996). Different AAV serotypes show distinct tissue tropism primarily determined by the availability and expression pattern of receptor/co-receptor (Nonnenmacher and Weber, 2012), including a common AAV receptor (AAVR) essential for particle entry (Pillay et al., 2016). Following endocytic uptake, AAV capsid translocates into the nucleus, where ssDNA genome is released and converted into transcriptionally

competent dsDNA genome. When a rAAV is used, the rAAV genome can be further processed to episomal circular forms that persist extrachromosomally in the nucleus and are responsible for long-term transgene expression (Duan et al., 1998).

A recent study by Lucifora et al. detected cccDNA in mice infected with rAAV carrying an 1.2-fold overlength HBV genome (Lucifora et al., 2017), which raised the question whether efficient nuclear import of rcDNA-containing capsids may be possible. To address this question, we infected wild-type (WT) C57BL/6 mice with our rAAV-HBV carrying an 1.3-fold overlength HBV genome (rAAV-HBV1.3) and analyzed cccDNA sequences detected in those mice. In addition, we investigated how the cccDNA-like molecules are formed and whether they are functional. Our results demonstrated that authentic cccDNA is established early after rAAV-mediated HBV genome delivery; however, intracellular HBV genome recycling does not result in cccDNA formation. We provide strong evidence that cccDNA is formed by intramolecular recombination based on >900 identical base pairs at 5' and 3' ends in the overlength HBV transgene. Furthermore, kinetic analysis of cccDNA formation and HBV antigen expression revealed that contribution of cccDNA for HBV gene expression is only minor.

2. Materials and methods

2.1. rAAV-HBV constructs, virus production and quantification

pAAV-HBV1.3-GtD was constructed by inserting an 1.3-fold HBV genome, genotype D, (GenBank accession number: V01460.1) amplified from the pT-HBV1.3WT plasmid into an AAV2 ITR containing plasmid by using *HindIII* and *SacI* restriction enzyme site. pAAV-HBV1.3-GtA, -GtB and -GtC constructs carrying HBV genotype A, B, or C were generated by replacing HBV genotype D sequence from pAAV-HBV1.3-GtD with the respective genotype sequence. HBV genotype A, B, and C sequences were obtained from following sources: pRVHBV1.5.A (genotype A; kindly provided by Volker Bruss, Helmholtz Zentrum München, Germany), pZDonor_N4214_B2 and pZDonor_N3825_C1 (genotype B and C, respectively; kindly provided by Dieter Glebe, University Hospital Giessen, Germany). Details of the molecular cloning strategy will be made available on request.

rAAV carrying the overlength HBV genome was produced by standard triple transfection method. HEK293T cells were transfected with HBV-encoding AAV transfer plasmid (pAAV-HBV1.3), AAV packing plasmid (pXR8) and adenovirus helper plasmid (pXX6-80) by using linear polyethylenimine (Polysciences, Hirschberg an der Bergstrasse, Germany). After 72 h transfection, cells were lysed by three freeze-thaw cycles in lysis buffer (50 mM Tris-HCl [pH7.5], 150 mM NaCl, and 5 mM MgCl₂). Each cycle cells were frozen at –80 °C for 15 min and thawed at 37 °C for 15 min. The resulting cell lysate was treated with benzonase (SIGMA, Steinheim, Germany) at 37 °C for 30 min and was subjected to iodixanol gradient ultracentrifugation. rAAV was recovered from 40% iodixanol layer and titrated with quantitative PCR (qPCR) using AAVpro Titration Kit (for Real Time PCR) Ver.2 (Takara Bio, Saint-Germain-en-Laye, France) according to the manufacturer's protocol to determine vector genome equivalents (GE). The titer of rAAV-HBV1.3 virus stocks usually ranged from of 1×10^{11} to 1×10^{12} GE/ml.

2.2. Mice procedure and ethical statement

Male C57BL/6 mice were purchased at 8–10 weeks of age from Janvier Labs (Le Genest-Saint-Isle, France) and were kept under specific-pathogen-free (SPF) conditions at the in-house animal facility. Mice were injected with an rAAV-HBV1.3 vector or a recombinant adenoviral vector carrying an 1.3-fold overlength HBV genome (rAd-HBV1.3) diluted in PBS to a final volume of 100 μ l via the tail vein route (Sprinzl et al., 2001). rAAV-HBV1.3 containing HBV sequence from genotype D was used unless indicated otherwise. Mice were intravenously injected with an rAAV-HBV1.3 vector at a dose of 1.6×10^{10} , 5×10^{10} or $1 \times$

10¹¹ GE (two or three mice/group) allowing cccDNA detection and quantification by Southern blot analysis. HBV-transgenic (tg) mice (strain HBV1.3.32; kindly provided by Francis V. Chisari) were used in this study (Guidotti et al., 1995). Mice were weighed weekly and blood samples were collected from the submandibular vein by using a lancet regularly for the analysis of serum HBeAg and alanine aminotransferase (ALT) levels. Mice were euthanized by cervical dislocation at the indicated time points.

Animal experiments were conducted in accordance to the German regulations of the Society for Laboratory Animal Science (GV-SOLAS) and the European Health Law of the Federation of Laboratory Animal Science Associations (FELASA). Experiments were approved by the local Animal Care and Use Committee of Upper Bavaria (permission no.: 55.2-1-54-2532-112-13, 55.2-1-54-2532-57-14, and ROB-55.2-2532.Vet_02-17-227). Mice were kept under SPF conditions at biosafety level 2 animal facilities following institutional guidelines.

2.3. Southern blot analysis of cccDNA and capsid-associated HBV DNA

A modified Hirt extraction procedure was used to isolate protein-free forms of DNA, including cccDNA, as described previously (Ko et al., 2019; Yan et al., 2012). Briefly, mouse liver tissue (ca. one-seventh of the left lobe) were homogenized using a Dounce homogenizer or plastic pestles in 1.9 ml of lysis buffer (50 mM Tris-HCl [pH 7.5], 150 mM NaCl, 10 mM EDTA), and 100 µl of 20% SDS was added. After incubation at 37 °C for 1 h with gentle agitation, the lysate was mixed with 500 µl of 2.5 M KCl and incubated at 4 °C overnight. Hirt DNA was extracted by phenol-chloroform extraction and dissolved in TE buffer (10 mM Tris-HCl [pH 8.0], 1 mM EDTA). 20–50 µg of mouse Hirt DNA from each sample were separated by electrophoresis through an agarose gel and transferred onto a nylon membrane. The membrane was hybridized with a DIG-labeled probe in hybridization buffer (500 mM sodium phosphate buffer [pH 7.2], 1% BSA, 7% SDS, 1 mM EDTA) for 16 h at 65 °C. Images were obtained using DIG Luminescent Detection Kit (Roche) and Chemocam Imager (Intas, Göttingen, Germany). Multi Gauge software (Ver3.0, Fujifilm) was used to quantify the relative levels of cccDNA and other DNA species.

To determine the identity of cccDNA, Hirt-extracted DNA was either digested with restriction enzymes (FastDigest restriction enzymes by Thermo Fisher Scientific, Waltham, MA, USA) at 37 °C for 30 min or treated with T5 exonuclease (0.5 unit; NEB, Frankfurt, Germany) for 30 min or exonuclease I/exonuclease III (20 unit/25 unit; NEB) for 2 h at 37 °C before gel electrophoresis (Ko et al., 2018; Luo et al., 2017).

HBV and AAV-specific probes were generated by PCR using FastStart High Fidelity PCR System (Roche) and PCR DIG Labeling Mix (Roche). For HBV DNA probe, primers HBV89-F and HBV3090-R were used to make a 3 kb DIG-labeled PCR product with following PCR cycling conditions: 30 cycles of 95 °C denaturation for 30 s, 60 °C annealing for 30 s, and 72 °C extension for 150 s (Supplementary table S1). For probes detecting AAV nucleic acids, two primer sets were used to generate DIG-labeled PCR products recognizing 5'ITR and 3'ITR regions, respectively: 5ITR-F & 5ITR-R and 3ITR-F & 3ITR-R (Supplementary table S1). Amplification of 284 bp (for 5'ITR) and 427 bp (for 3'ITR) products were conducted by 30 cycles of 95 °C denaturation for 30 s, 55 °C annealing for 30 s, and 72 °C extension for 30 s. In addition to PCR products at correct size, truncated amplicons were detected, most likely due to palindromic sequences. PCR products including truncated amplicons were purified using High Pure PCR Product Purification Kit (Roche) and a 1:1 mixture by amount of those two ITR probes was used for Southern blot hybridization (Fig. S1).

A DIG-labeled mitochondrial DNA (mtDNA) probe was generated as a loading control of Hirt-extracted DNA. Briefly, mitochondrial gene fragment (nt 4350–5470; NCBI RefSeq: NC_012920.1) containing partial NADH dehydrogenase subunit 2 (MT-ND2) gene was amplified by PCR using Hirt-extracted DNA obtained from HepG2 cells and inserted into pcDNA1/Amp vector by using *Bam*HI and *Xho*I restriction enzyme sites.

The resulting pcDNA1/Amp-MT-ND2 plasmid was used as the template for DIG-labeled mitochondrial probe generation with following primers: MT4350-F and MT5470-R (Supplementary table S1). Due to supercoiling of mitochondrial genome, smear bands were observed by Southern blot detection that unwound after digestion by *Hind*III and resulted in detection of a linear fragment.

To prepare intracellular capsid-associated HBV DNA (rcDNA and replication intermediates), mouse liver tissue was lysed with core lysis buffer (50 mM Tris-Cl [pH 8.0], 100 mM NaCl, 1 mM EDTA, 1% NP-40) at 4 °C for 1 h. After centrifugation at 12,000g for 15 min, the cytoplasmic lysate (3 mg) was further processed as described elsewhere for Southern blot analysis (Ko et al., 2014).

2.4. Sequencing analysis

To analyze cccDNA sequence, DNA extracted after a Hirt method was treated with T5 exonuclease and cccDNA was extracted from an agarose gel following gel electrophoresis. Four different sets of primers were used to generate PCR products (552, 1815, 1504, 1040 bp) and those cccDNA amplicons were analyzed by Sanger sequencing.

To analyze the sequence of HBV 5' C ORF in all episomal DNA species of rAAV-HBV1.3-C-null (5') infected mice, Hirt-extracted DNA was treated with T5 exonuclease and a PCR amplicon was generated using primers HBV3022-F and HBV246-R (Supplementary table S1). To have sequence of HBV 5' C ORF in cccDNA, cccDNA was prepared as for the Sanger sequencing analysis and subjected to PCR reaction with primers HBV 3022-F and HBV246-R. The resulting products were analyzed by Illumina Sequencing. DNA library preparations, sequencing reactions, and adapter sequences trimming were conducted at GENEWIZ, Inc. (South Plainfield, NJ, USA). DNA library preparation was performed using NEBNext Ultra DNA Library Prep kit following the manufacturer's recommendations (Illumina, San Diego, CA, USA). Briefly, end repaired adapters were ligated after adenylation of the 3'ends followed by enrichment by limited cycle PCR. DNA libraries were validated and quantified before loading. The pooled DNA libraries were loaded on the Illumina instrument according to manufacturer's instructions. The samples were sequenced using a 2 × 250 paired-end (PE) configuration. Image analysis and base calling were conducted by the Illumina Control Software on the Illumina instrument.

2.5. Western blot analysis of HBV core protein

Mouse liver tissue was lysed in RIPA buffer (50 mM Tris-Cl [pH 8.0], 100 mM NaCl, 1 mM EDTA, 0.5% sodium deoxycholate, 0.1% SDS, 1% NP-40, protease inhibitor cocktail) at 4 °C for 1 h. After centrifugation, whole liver lysate (50–100 µg) was subjected to SDS-PAGE followed by immunoblotting using an anti-core antibody (in-house 8C9 mouse hybridoma supernatant generated against HBV core peptide⁷⁵⁻⁸⁶) and anti-actin antibody (SIGMA, Steinheim, Germany). All blots were developed using ECL Prime Western Blotting Detection Reagent (GE Healthcare, Freiburg, Germany).

2.6. Native agarose gel electrophoresis of HBV capsid

Native agarose gel electrophoresis was performed as described previously (Ko et al., 2019). Briefly, mouse liver tissue was homogenized in lysis buffer (50 mM Tris-Cl [pH 8.0], 100 mM NaCl, 1 mM EDTA, and 1% NP-40) at 4 °C for 1 h and centrifuged at 12,000g for 15 min. The resulting cytoplasmic liver lysate (50–100 µg) was directly separated into an 1.2% agarose gel and transferred onto a PVDF membrane in 10x SSC buffer (1.5 M NaCl, 150 mM sodium citrate). Capsids were visualized by Western blot procedure with an anti-core antibody (Cell Marque, Rocklin, California, USA).

2.7. Detection of serum HBeAg and HBsAg

The levels of HBeAg and HBsAg in mouse sera were measured using the automated Architect instrument (Abbott Laboratories, Hannover, Germany) (Michler et al., 2020).

2.8. Immunohistochemistry (IHC)

Liver tissues were fixed in 4% paraformaldehyde for 48 h and paraffin embedded. Tissue sections were subjected to staining of HBV core protein using an automated Bond-Max IHC system (Leica Biosystems), as previously described (Kosinska et al., 2019). Briefly, 2 μ m liver sections were incubated with a rabbit polyclonal antibody against HBV core protein (Origene #AP10430PU-N; diluted 1:50) followed by peroxidase-coupled secondary anti-rabbit IgG antibody and peroxidase staining. Slides were scanned using an SCN400 slide scanner (Leica Biosystems). The number of core protein positive hepatocytes were

manually counted in 3–5 random vision fields per sample (40 \times magnification).

3. Results

3.1. rAAV-HBV1.3 infected mice support HBV cccDNA formation

Given that mice intravenously infected with rAAV-HBV carrying an 1.2-fold overlength HBV genome (genotype D) support cccDNA formation (Lucifora et al., 2017), we wanted to confirm this finding. To achieve high level HBV gene expression, we used an 1.3-fold overlength HBV genome (genotype D, ayw) including HBV enhancer I positioned at its 5' termini (Guidotti et al., 1995). For efficient liver-directed HBV genome delivery, AAV serotype 8 capsid pseudotyped with ITRs from AAV serotype 2 genome (AAV2/8) was used (Davidoff et al., 2005; Thomas et al., 2004). Southern blot analysis of Hirt-extracted DNA detected cccDNA in the size of a 2.1-kb from liver tissue of a mouse

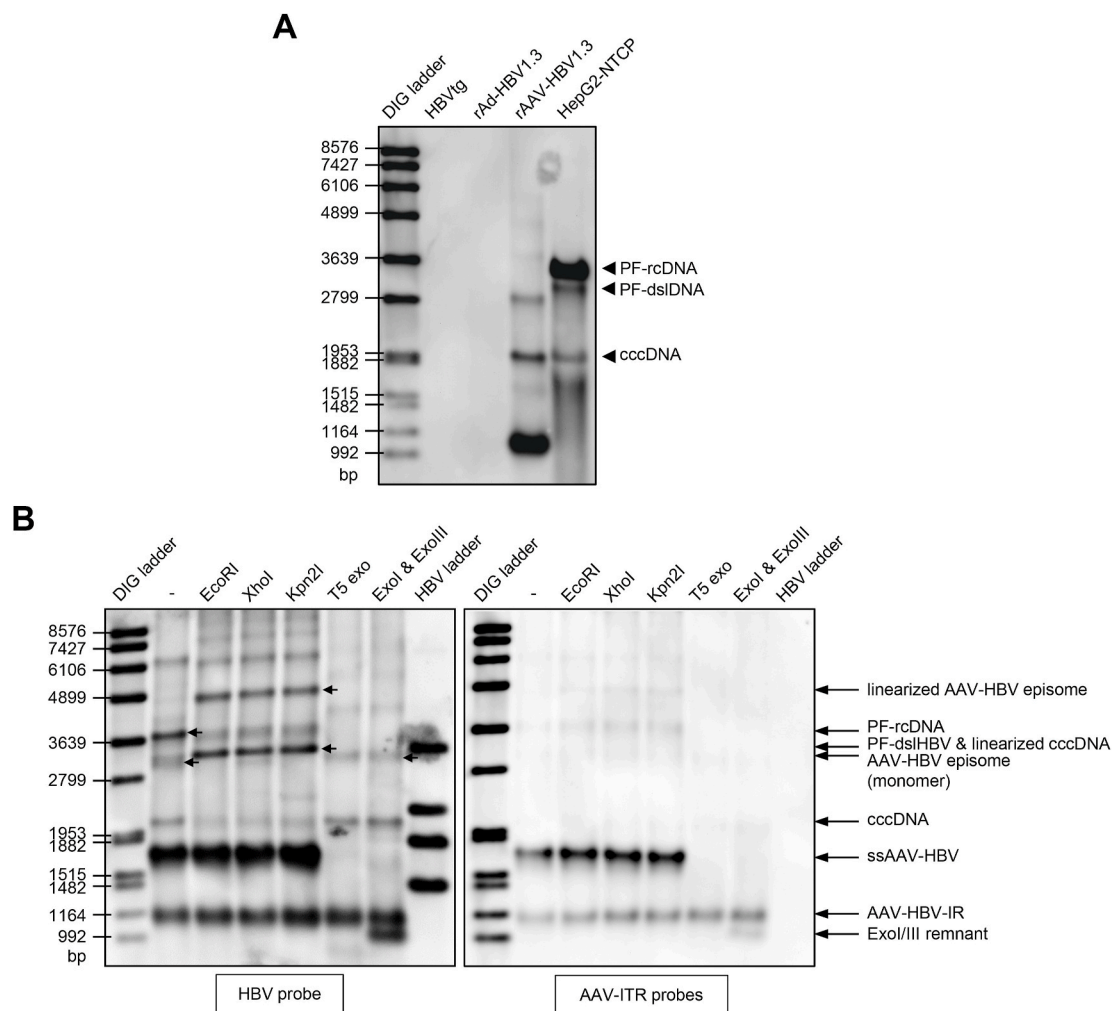


Fig. 1. Analysis of cccDNA formation in different HBV mouse models. (A) C57BL/6 mice were intravenously injected with either rAAV-HBV1.3 vector (5×10^{10} GE/mouse) or rAd-HBV1.3 vector (2×10^9 infectious units/mouse) and were sacrificed after 4 weeks together with an HBV-transgenic mouse. Liver tissues were collected and subjected to a modified Hirt extraction (see methods). Hirt-extracted DNA from HBV-infected HepG2-NTCP-K7 cells were included as a positive control. Hirt-extracted DNA (25 μ g) from each sample was analyzed by Southern blotting using a digoxigenin (DIG)-labeled HBV-specific DNA probe. DIG-labeled DNA fragments (8576–992 bp) were used as molecular weight standards. (B) rAAV-HBV1.3 vector was injected intravenously to a C57BL/6 mouse at a dose of 1×10^{11} GE. The mouse was sacrificed at 4 weeks post-injection and intrahepatic DNA was extracted by a modified Hirt method. The isolated Hirt DNA was either left untreated or treated with a restriction enzyme or exonuclease(s) as indicated and separated into two agarose gels for Southern blot analysis. After being transferred to nylon membranes, one membrane was hybridized with an HBV probe and the other membrane was probed with AAV-ITR probes. GE, vector genome equivalents; HBVtg, HBV-transgenic; PF, protein-free; rc, relaxed circular; dsI, double-stranded linear; ssAAV-HBV, single-stranded AAV-HBV DNA; AAV-HBV-IR, DNA species most likely resulting from intramolecular recombination of a double-stranded AAV-HBV1.3 genome that containing AAV and HBV sequences; T5 exo, T5 exonuclease; ExoI & ExoIII, exonuclease I and III; bp, base pair.

infected with rAAV-HBV1.3 and from HepG2-NTCP cells infected with HBV as a positive control (Fig. 1A). A modified Hirt extraction method allows enrichment of extrachromosomal, protein-free DNA species, such as viral episomes and mitochondrial DNA (Hirt, 1967; Yan et al., 2012). In contrast, cccDNA was neither detected in HBVtg mice nor in mouse livers in which hepatocytes were transduced with an adenoviral vector transferring the same 1.3-fold overlength HBV genome (Fig. 1A) (Sprinzl et al., 2001).

To test the identity of cccDNA, we treated Hirt-extracted DNA with either restriction enzymes recognizing a single-site on the cccDNA or indicated exonucleases, and performed Southern blot analysis with probes specifically binding to the HBV sequence or the ITR2 sequences (Fig. 1B). Restriction enzyme *EcoRI*, *XhoI*, or *Kpn2I* linearized cccDNA giving rise to a 3.2-kb double-stranded linear form. As expected, cccDNA was resistant to T5 exonuclease treatment and a combinatorial treatment of exonuclease I and exonuclease III (Ko et al., 2018; Luo et al., 2017), indicating the covalently-closed and supercoiled nature of cccDNA.

We observed HBV- and/or AAV-specific DNA species migrating distinctly (Fig. 1B). The intensity of AAV-HBV bands was lower when a membrane was hybridized with the ITR probes, likely due to a shorter probe size together with the complex secondary structure of the ITRs. Protein-free (PF) forms of HBV replication intermediates i.e. PF-rcDNA and PF-double-stranded linear (dsl)HBV were detected. Circular AAV-HBV double-stranded (ds) monomer (termed AAV-HBV episome) comigrated with a 3.2-kb HBV size marker and converted to a molecular weight of approximately 4.8 kb following restriction enzyme digestion, as reported previously (Lucifora et al., 2017). A restriction enzyme-resistant, but exonuclease-sensitive DNA species of approximately 1.6 kb is single-stranded (ss) AAV-HBV genomes (ssAAV-HBV), as evidenced by comigration with input vector genomes isolated from rAAV2/8 capsids (Fig. S2). Interestingly, we noted a DNA species resistant to restriction enzyme and exonuclease digestion and migrating at the position of a 1.1 kb, suggesting an episomal DNA containing partial HBV and ITR2 sequences (named by AAV-HBV-IR; see discussion for the identity of this molecule). Following restriction enzyme digestion, we observed high-molecular weight HBV- and AAV-specific bands appearing at >6 kb. These bands are likely originated from AAV-HBV head-to-tail concatemers (Lucifora et al., 2017). Exonuclease I and III

treatment showed the same picture as T5 exonuclease except a new faster-migrating band. This ~1 kb band could represent DNA remnants made up of HBV and AAV fragments due to inadequate digestion.

Taken together, our findings confirm cccDNA formation in rAAV-HBV infected mice and show that rAAV-HBV infection but neither rAd-HBV infection nor an HBV transgene results in cccDNA formation. This suggests that an rAAV-driven mechanism specifically induces cccDNA genesis.

3.2. cccDNA is formed in rAAV-HBV1.3 infected mice bearing different HBV genotypes

HBV can be divided into nine genotypes (A to I) which show a distinct global distribution (Velkov et al., 2018). cccDNA formation was so far only shown by an AAV-mediated delivery of HBV genotype D (Lucifora et al., 2017). We wondered if cccDNA can also be formed when other HBV genotypes are delivered by the same rAAV2/8 vector. When C57BL/6 mice were intravenously infected with rAAV-HBV1.3 harboring any of the HBV genotypes A, B, C, or D, cccDNA as well as serum HBeAg and HBsAg were detected in the livers of all animals (Fig. 2A and data not shown). The difference in cccDNA levels among HBV genotypes may reflect a modest difference of probe binding affinity, as the HBV-specific DNA probe was generated using an HBV genotype D template, or variation in infectivity of the different rAAV-HBV stocks or differences in the recombination efficiency between different HBV genotypes. When mice were infected with rAAV-HBV1.3 (genotype D) at a dose of 1.6×10^{10} GE, the number of HBV core protein positive hepatocytes was approximately 24% (Fig. 2B); infection rate was increased to approx. 58% when infected at a dose of 1×10^{11} GE (data not shown). Taken together, our results demonstrate that cccDNA is formed independent of the HBV genotype transferred by the rAAV-HBV1.3.

3.3. rAAV-HBV1.3 infected mice establish authentic cccDNA

Southern blot analysis of Hirt extracted DNA in combination with restriction enzyme or exonuclease allowed us to detect intrahepatic cccDNA. However, this approach relied on the biochemical property and migration pattern of cccDNA on the agarose gel. Thus, we cannot rule

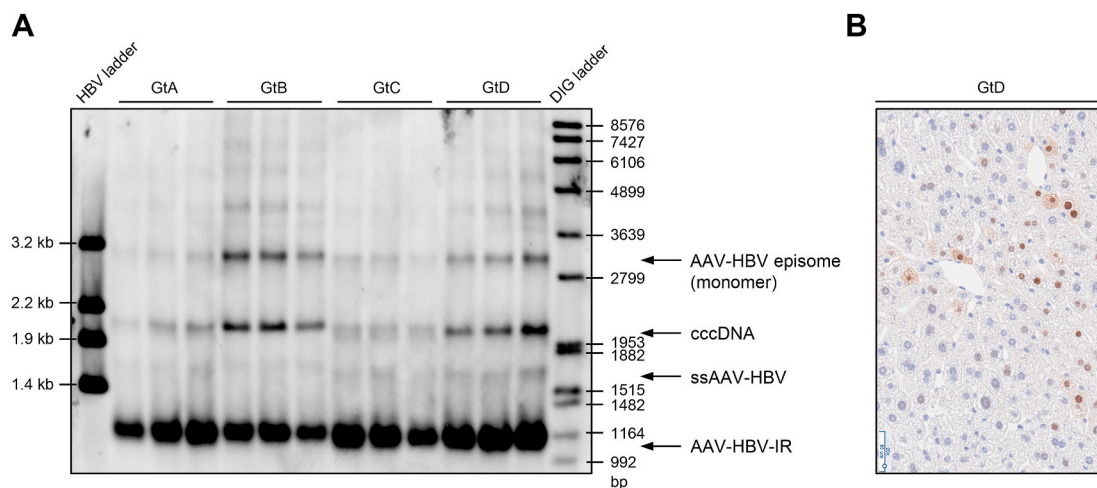


Fig. 2. Analysis of cccDNA formation and core protein expression in mice infected with rAAV-HBV1.3 carrying different HBV genotypes. (A) rAAV vectors carrying an 1.3-fold overlength HBV genome of genotype A, genotype B, genotype C, or genotype D were administered by intravenous route to C57BL/6 mice at a dose of 1.6×10^{10} GE ($n = 3/\text{group}$). Southern blot analysis of intrahepatic Hirt-extracted DNA was performed at day 28 after infection. Both restriction fragments derived from HBV genome (first lane of the gel) and DIG-labeled DNA fragments (last lane of the gel) were used as size marking ladders. (B) Intrahepatic HBV core protein was visualized by immunohistochemical staining of liver tissue transduced with rAAV-HBV1.3 (genotype D) using a polyclonal rabbit anti-HBV core antibody (Origen, #AP10430PU-N) preferentially recognizing HBV core protein derived from genotype D. GE, vector genome equivalents; ssAAV-HBV, single-stranded AAV-HBV DNA; AAV-HBV-IR: DNA species most likely resulting from intramolecular recombination of a double-stranded AAV-HBV1.3 genome that containing AAV and HBV sequences; bp, base pair; Gt, genotype.

out the possibility of cccDNA sequence alteration, such as short fragment insertion or deletion, which cannot be observed by Southern blotting. To determine the integrity of cccDNA, we analyzed the sequence of cccDNA PCR amplicons and compared it to cccDNA sequence established in human hepatocytes upon infection (Fig. S3A). To ensure specific amplification of cccDNA, we eliminated other HBV DNA species (e.g., rcDNA and HBV replication intermediates) by treating intrahepatic Hirt-extracted DNA with T5 exonuclease and isolated cccDNA from agarose gel slices. The resulting DNA was subjected to either conventional PCR or qPCR reaction with four different primer sets. Sanger sequencing analysis of cccDNA amplicons showed a perfect match of those amplicon-derived sequences to genuine cccDNA sequences established in HBV-infected human hepatocytes (Fig. S3A). As an example, the sequence alignment of a cccDNA-selective qPCR product to authentic cccDNA is shown in Fig. S3B. Overall, our results demonstrated that rAAV-HBV infected mice produce cccDNA in mouse hepatocytes.

3.4. Intramolecular homologous recombination is responsible for cccDNA formation early after AAV-HBV1.3 genome delivery

We next investigated how cccDNA is formed in AAV-HBV mouse model. There are two plausible ways of cccDNA genesis: (i) cccDNA is formed early after AAV-HBV genome delivery by recombination based on identical sequences in the 1.3-fold overlapped HBV transgene (model 1) or (ii) cccDNA is established after nuclear reimport of HBV rcDNA formed within HBV capsids (model 2) (Fig. 3A). To investigate this, we generated two different core protein-deficient rAAV-HBV1.3-C-null variants by introducing premature stop codons in both, 5' and 3' core gene open reading frames (C-ORF), or only in the 5' C-ORF and analyzed cccDNA formation at week 1 and week 4 post-injection (Fig. 3B). Introducing two stop codons at amino acid positions 6 and 7 in the 5' C-ORF would result in premature termination of core protein and HBV e antigen (HBeAg) translation which stems from the same Pre-C/C-ORF. Because HBV generates its rcDNA genome by reverse transcription inside a newly formed capsid, the usage of C-null variants allows us to exclude the possibility of intracellular HBV genome recycling in contributing to cccDNA formation and to obtain an insight into the origin of cccDNA.

Southern blot analysis detected cccDNA in mice infected with rAAV-HBV-C-null variants at week 1 (Fig. 3C) and week 4 post-infection (data not shown). Levels of cccDNA were higher in mice infected with rAAV-HBV1.3-C-null (5'&3') compared to the WT. At present, the modest difference in cccDNA levels observed between different rAAV-HBV1.3 genotypes is unclear. In an analogous experiment, we were able to detect intrahepatic cccDNA as early as 3 days post-infection (Fig. S4). This shows that cccDNA is established early after AAV-HBV genome transfer and cccDNA formation is independent of core protein expression and therefore independent of HBV replication.

As expected, mice infected with rAAV transferring an HBV genome in which both C-ORFs were knocked-out (rAAV-HBV1.3-C-null (5'&3')) did neither express core protein or form capsid (Fig. 3D) nor support HBV replication, as evidenced by a lack of rcDNA and HBV replication intermediates (Fig. 3E). Interestingly, intrahepatic core protein expression was partially restored when mouse hepatocytes were transduced with an HBV construct in which the truncated 3' C-ORF remained intact (rAAV-HBV1.3-C-null(5')) (Fig. 3D). Similarly, serum HBeAg expression was abrogated in mice that had received AAV-HBV1.3-C-null (5'&3'), while HBeAg was detected at levels of about one-third of the WT in those that had received rAAV-HBV1.3-C-null (5') (Fig. 3F). Of note, hereby, core protein and HBeAg can only be translated if the 5' C-ORF is restored as 3' C-ORF is incomplete (Fig. 3B). Indeed, next generation sequencing analysis of the 5' C-ORF of all episomal species and cccDNA in rAAV-HBV1.3-C-null (5') infected mice showed reversion to WT sequence (Fig. 3G) at 8.6% and 38.8%, respectively, suggesting that homologous recombination allows restoration of the C-ORF. In summary, our results support the notion that the cccDNA detected in livers of mice infected

with rAAV-HBV is a product of recombination based on HBV-sequence homology.

3.5. cccDNA is not the major template for HBV gene expression in rAAV-HBV1.3 infected mice

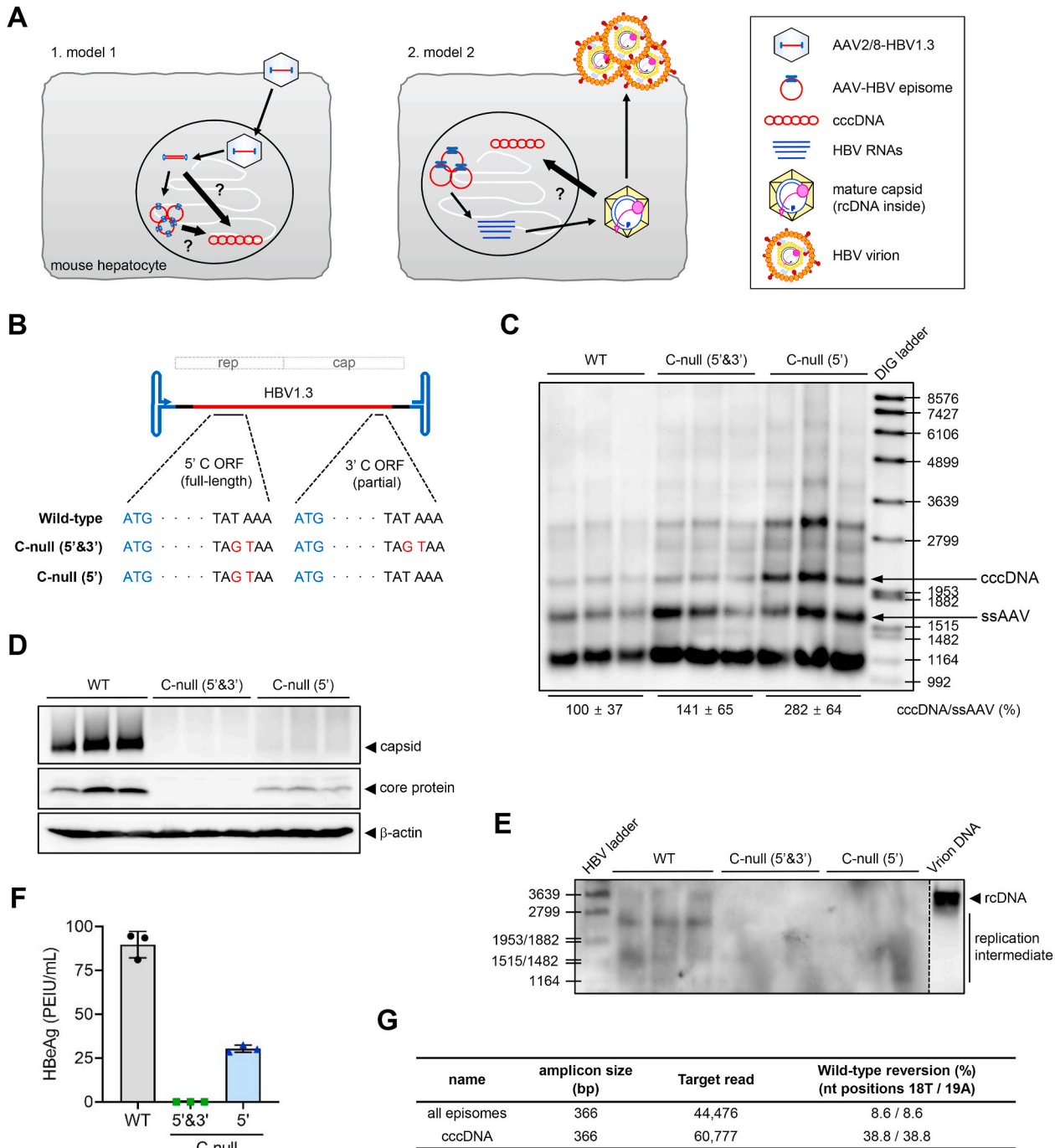
Circularized episomal forms (monomer, dimer, and concatemer) of AAV-transgene enable persistent transgene expression in the liver (Nakai et al., 2000). We sought to examine whether cccDNA is maintained in the nucleus of mouse hepatocytes and to which extent cccDNA and the AAV-HBV episomes contribute to HBV gene expression over time. We performed a kinetics experiment where mice were sacrificed 1, 2 and 4 weeks after rAAV-HBV1.3-WT vector transfer and the liver tissues were analyzed for cccDNA formation. In parallel, we monitored serum HBeAg levels as an indicator of transgene expression. As shown in Fig. 4A, cccDNA levels were highest at week 1 post-infection and gradually decreased over time. At week 4, cccDNA levels had dropped by 76%–34% of the level determined at week 1. When mice were sacrificed at week 8 in an analogous experiment, cccDNA levels had dropped to 28% detected in those sacrificed after at week 1 (Fig. 4B). In contrast to decreasing cccDNA levels, constant amounts of mitochondrial DNA used as a loading control were detected, and the monomeric AAV-HBV episome forming early after infection was not significantly decreased (Fig. 4B) or even modestly increased (Fig. 4A). Serum HBeAg levels peaked at week 2 post-infection and remained stable throughout the experiment until week 8 (Fig. 4). Due to spontaneous anti-HBs seroconversion and HBsAg clearance occurring in some mice infected with a high dose of rAAV-HBV inoculum ($>1.6 \times 10^{10}$ GE), serum HBsAg levels was not regarded a suitable marker for transgene expression (Fig. S5). In summary, these data indicate a limited contribution of cccDNA to HBV gene expression in the AAV-HBV mouse model and confirm that circularized episomal AAV-HBV genomes are persistent, functional templates for HBV gene expression and viral replication.

4. Discussion

Lack of convenient animal models supporting the complete HBV life cycle is a major hurdle of HBV studies. Animal models are required when it comes to understanding the complex virus-host interactions and the development of immune therapies. While identification of the HBV uptake receptor allowed establishing cell lines that replicate HBV from its natural transcription template, immune competent animal models supporting the full HBV life cycle are still lacking (Protzer, 2017). HBVtg mice serve as surrogate model for HBV infection as do mice injected with replication-competent HBV genomes either using hydrodynamic injection of DNA or adenoviral or AAV vectors. Of note, none of these models support *de novo* cccDNA formation. A recent study reporting cccDNA detection in mouse liver infected with an rAAV-HBV vector (Lucifora et al., 2017) brought up the questions as to whether it is authentic cccDNA, how it is formed and whether it is functional.

We confirmed cccDNA formation in the liver of C57BL/6 mice following rAAV-mediated HBV genome transfer. Susceptibility of the cccDNA molecules to restriction enzymes and resistance to exonucleases provided strong biochemical evidence of cccDNA establishment in rAAV-HBV infected mouse model. Sequence analysis of cccDNA amplicons generated by PCR reactions of T5 exonuclease-treated, gel-purified cccDNA demonstrated that this molecule is identical to cccDNA established in human hepatocytes following *de novo* HBV infection. Our results demonstrate that authentic cccDNA is synthesized and represents the dominant population although we cannot rule out the existence of some cccDNA-like molecules with sequence alteration.

Several lines of evidence support the notion that intramolecular recombination is responsible for cccDNA genesis early after rAAV-mediated HBV genome delivery into the nucleus. Firstly, core protein-deficient rAAV-HBV1.3-C-null vector transfer resulted in cccDNA formation. Since HBV DNA synthesis takes place within the newly-



(caption on next page)

Fig. 3. Analysis of cccDNA formation in mice infected with rAAV-HBV1.3 C-null variants. (A) Schematics illustrating two potential mechanisms leading to cccDNA generation in rAAV-HBV1.3 infected mice. cccDNA could be formed by homologous recombination early after the single-stranded rAAV-HBV1.3 genome has been delivered into the nucleus and converted into double-stranded forms (model 1, left). cccDNA could also be formed by reimport of HBV rcDNA-containing mature capsids into the nucleus at a later stage (model 2, right). (B) Illustration showing a single-stranded AAV-HBV genome carrying a 1.3-fold overlength HBV genome. The two open reading frames (ORFs) encoding nonstructural proteins (rep) and structural proteins (cap) are replaced with an 1.3-fold overlength HBV genome (~4.1 kb; colored red) and short plasmid-derived sequences (~450 bp colored black), leaving two T-shaped ITRs (~150 bp, each; colored blue) at the ends. The position of HBV 5' C-ORF (full-length) and 3' C-ORF (partial) are denoted. Start codon is highlighted in blue and single-base substitutions at amino acid positions 6 and 7 resulting in pre-mature stop codons of core protein sequence are indicated in red either within both C-ORFs (C-null (5' & 3')) or within the 5' C-ORF only (C-null (5')). (C–G) Three groups of mice (n = 3/group/time point) were injected with rAAV-HBV1.3 (1.6 × 10¹⁰ GE/mouse) carrying wild-type HBV genome, C-null (5' & 3') variant, or C-null (5') variant. Mice were sacrificed on day 7 (C) or day 28 (D–G) post-infection and liver and serum samples were collected. (C) DNA was extracted the Hirt method from liver samples at day 7 post-infection and cccDNA was detected by Southern blotting. DIG-labeled DNA fragments serve as a size marking ladder. (D) Intrahepatic capsid and core protein were detected by native agarose gel electrophoresis and Western blot analysis, respectively. After capsid visualization, the membrane was *in situ* hybridized with an HBV DNA probe to detect HBV DNA packaged within capsids. β-actin was used as a loading control. (E) HBV DNA (rcDNA and replication intermediates) were isolated from intrahepatic HBV capsids and analyzed by Southern blotting using an HBV DNA probe. (F) Serum HBeAg levels were measured using a diagnostic assay. (G) Next-generation amplicon sequencing of 5' C-ORF. Hirt DNA was isolated from livers of rAAV-HBV1.3-C-null (5') infected mice and treated with T5 exonuclease to obtain episomal DNA species. Additionally, T5 exonuclease-treated Hirt DNA was separated through an agarose gel and DNA migrating at a position of ~2.1 kb was isolated to obtain HBV cccDNA. PCR amplicons were generated from all episomal DNAs (cccDNA, double-stranded AAV-HBV monomer/dimer/concatemer genomes) or cccDNA using primer HBV3022-F and HBV246-R and analyzed by Illumina sequencing. Amplicon size, number of sequencing reads, and percentage of reversion to the wild-type at nucleotide positions 18 and 19 are shown. GE, vector genome equivalents; rcDNA, relaxed circular DNA; WT, wild-type.

synthesized capsids, this result indicates that cccDNA formation in rAAV-HBV1.3 infected animals occurred independent of HBV core protein expression and replication. Secondly, cccDNA was detected as early as day 3 post-infection when HBV proteins and viral DNAs were barely detectable. Thirdly, cccDNA did not persist, but steadily decreased over time indicating a negligible role of intracellular HBV genome recycling. If cccDNA had been established by reimport of rcDNA into the nucleus, cccDNA would have appeared at later time points (>2 weeks) after the accumulation of mature capsids and would have increased or at least been maintained at constant levels.

Fourthly, we observed restoration of core protein expression and its respective coding nucleotide sequence to the WT when mice were infected with an rAAV-HBV1.3-C-null (5') vector in which stop codons were only introduced to 5' C-ORF, but not 3' C-ORF of the HBV transgene. In the absence of capsid formation and reverse transcription taking place within the capsids, this indicated that intramolecular recombination resulting in an exchange of mutated 5' by WT 3' HBV sequences must have occurred to restore the WT sequence. This is enabled by a 920-bp long identical HBV sequences present at both ends of the 1.3-fold, linear HBV transgene (Guidotti et al., 1995). This overlap is required to allow transcription of HBV RNAs under control of their natural promoter/enhancer elements and expression of all HBV proteins from a linear genome while the natural transcription template, the circular cccDNA, does not require these duplications.

Last but not least, we detected an episomal DNA species containing AAV and HBV sequences that we termed AAV-HBV-IR and that most likely resulted from intramolecular recombination. Intramolecular recombination in a dsAAV-HBV1.3 genome would result in two dsDNA products: (1) cccDNA (circular; 3.2 kb) and (2) remaining 5' and 3' AAV-HBV fragments(s) still containing overlapping AAV and HBV sequences (1.6 kb; circular or linear). It seems most likely that the HBV transgene folds on itself to juxtapose the 920-bp identical HBV sequences and this arrangement forms a loop of the intervening sequence and allows a cccDNA molecule to be excised. Indeed, we noted a species fast migrating in a gel (locating to approx. 1.1 kb) that was resistant to exonucleases and to a panel of restriction enzymes (*EcoRI*, *XhoI*, *Kpn2I*) cutting cccDNA. Interestingly, another set of restriction enzymes (*HindIII*, *SacI*, *BglII*) was capable of linearizing the AAV-HBV-IR species, yielding a 1.6 kb linear fragment (Fig. S6). These restriction sites are present in the AAV-HBV transgene, but not in cccDNA, indicating that cccDNA sequences had been removed. The stronger intensity of AAV-HBV-IR bands comparing to cccDNA bands may represent a more open structure of AAV-HBV-IR resulting in a better recognition by hybridization probes. An alternative explanation could be that AAV-HBV-IR is more stable than cccDNA due to the presence of AAV ITRs.

As rAAV exploits cellular DNA recombination and repair factors to

generate circular episomal products (Choi et al., 2006), it is reasonable to speculate that the HBV transgene is delivered into an environment enriched with those factors allowing intramolecular recombination. This may explain why rAd-HBV1.3 infected and HBVtg mice do not establish cccDNA, but rAAV-HBV1.3 transduced mouse hepatocytes do. We did neither further investigate the exact underlying molecular mechanism of cccDNA formation nor the host repair machineries involved. Unraveling the molecular mechanism seemed of minor importance to us because cccDNA formation in this model was not relevant for the HBV life cycle and it may be related to rAAV-HBV vector doses.

Considering that long-term transgene expression is associated with the persistence of episomal circularized forms of rAAV genomes (Duan et al., 1998; Nakai et al., 2000), it seemed important to determine the contribution of the cccDNA molecules formed by recombination to HBV gene expression. Previous studies have shown that cccDNA or cccDNA-like molecules (i.e., rcccDNA or HBVcircles) result in cccDNA-dependent viral gene expression when introduced into the mouse liver (Wang et al., 2017; Wu et al., 2020; Yan et al., 2017). This led us to hypothesize that both, rAAV-HBV episomes and cccDNA, contribute to persistent HBV gene expression. Because it was technically impossible to purify one template from the other, we performed a kinetics analysis of cccDNA and HBeAg expression to obtain information of the functionality of the cccDNA molecules. Unexpectedly, cccDNA levels rapidly dropped, whereas HBeAg levels reached a plateau at 2 weeks after rAAV-HBV1.3 infection and then remained at a constant level. This result provides indirect evidence that the persistence of HBeAg expression is primarily from rAAV HBV episomes and the cccDNA molecules formed only have a minor contribution.

In the livers of our rAAV-HBV1.3 infected mice, the estimated half-life of cccDNA was 16 days which is significantly shorter than the 40 days in HBV-infected hepatoma cells (Ko et al., 2018). In hepatitis B patients cccDNA half-life is even more prolonged (9.2 months) (Boyd et al., 2016) and exceeds the half-life of plasmid-derived, recombinant cccDNA in Alb-Cre tg mice (7.8 weeks) (Wu et al., 2020). This relatively short half-life could be explained by a subsequent intermolecular recombination event e.g. into the any rAAV-HBV molecules containing the 920-bp homologous sequence destroying the typical cccDNA structure. The detection of a new DNA species appearing from 2 weeks post-injection supports this hypothesis (Fig. S7). Alternatively, there might be murine host factors affecting cccDNA stability.

In summary, we have demonstrated that the transfer of replication-competent HBV genomes mediated by an rAAV-vector leads to intramolecular recombination and formation of authentic HBV cccDNA in the mouse liver. Although the cccDNA molecules cannot be distinguished from their natural counterparts they are not formed by intracellular HBV genome recycling occurring during natural HBV infection but by DNA

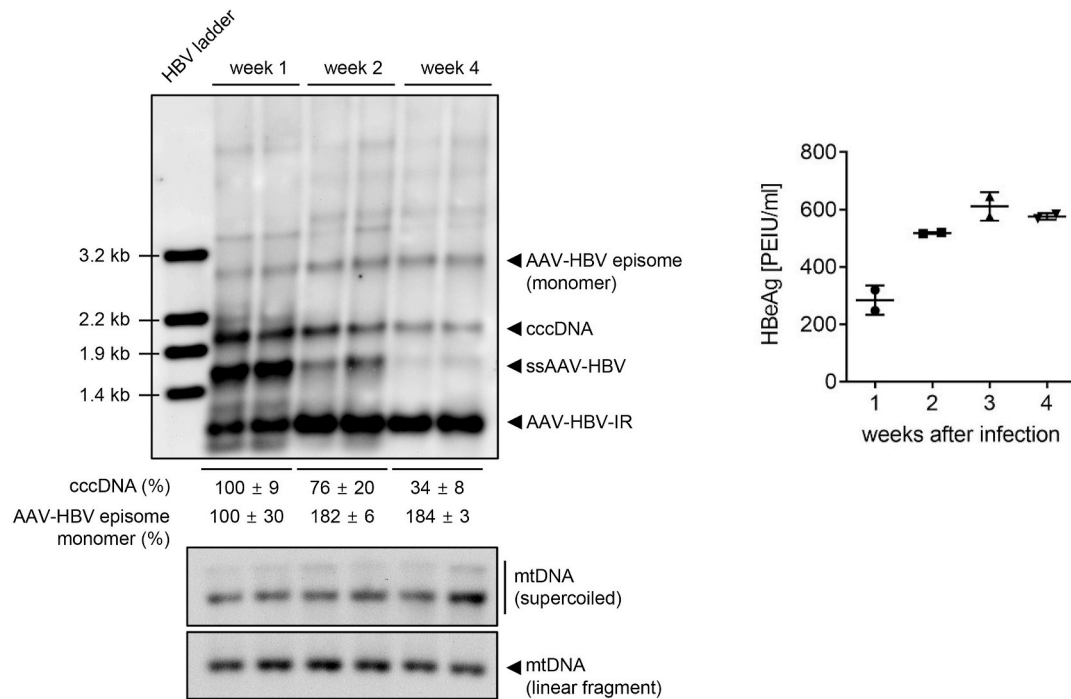
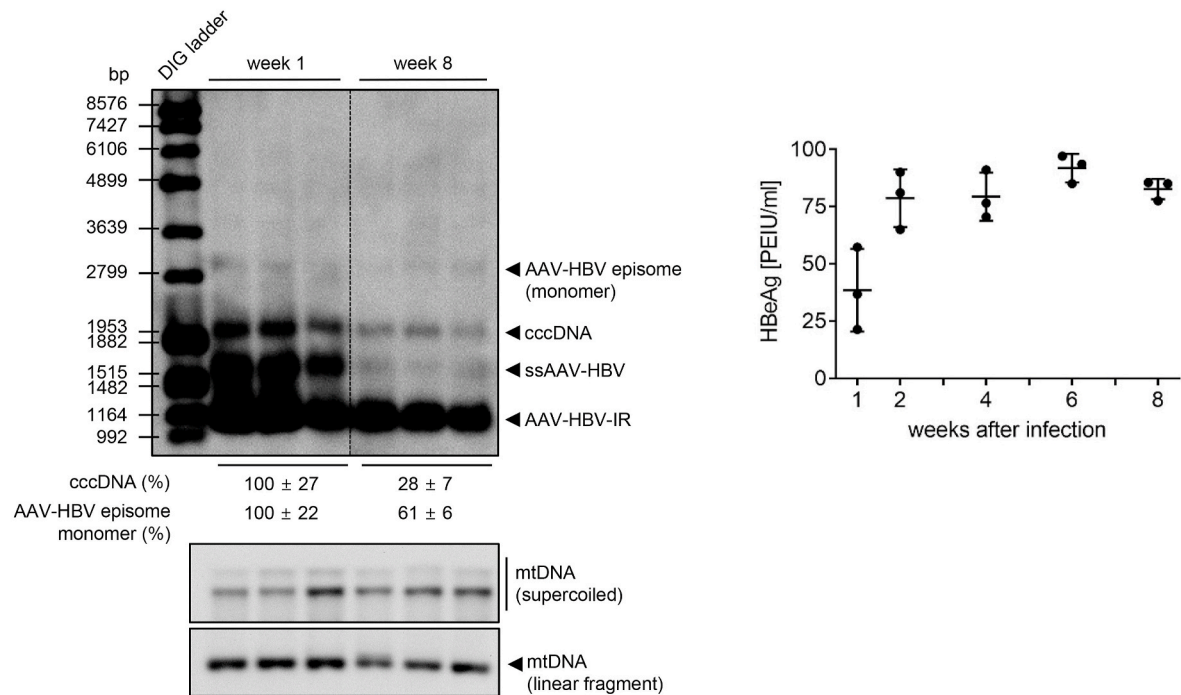
A**B**

Fig. 4. Kinetics analysis of cccDNA formation and serum HBeAg level in rAAV-HBV1.3 infected mice. (A) Six C57BL/6 mice were intravenously injected with an AAV vector harboring a 1.3-fold overlength HBV genome at a dose of 5×10^{10} GE/mouse. Two mice were sacrificed at 1, 2 and 4 weeks post-injection, respectively. Intrahepatic cccDNA levels were determined at indicated time points. DNA (50 μ g) extracted using the Hirt method from liver tissue was subjected to Southern blot analysis using an HBV-specific probe. cccDNA bands were quantified relative to those detected at week 1. Kinetics of serum HBeAg levels are shown on the right. Mean \pm standard deviation is given. Mitochondrial DNA was hybridized as a loading control. (B) Six C57BL/6 mice were injected at a dose of 1.6×10^{10} GE/mouse of rAAV-HBV1.3 and three animals each were sacrificed after one and eight weeks. Intrahepatic cccDNA levels and serum HBeAg levels were analyzed as described for panel A. For both experiments, mice were regrouped based on HBeAg titer measured at day 7 post-infection and sacrificed at the indicated time points. GE, vector genome equivalents; ssAAV-HBV, single-stranded AAV-HBV DNA; AAV-HBV-IR: DNA species most likely resulting from intramolecular recombination of a double-stranded AAV-HBV1.3 genome that containing AAV and HBV sequences; bp, base pair; mtDNA, mitochondrial DNA.

recombination events. We showed that cccDNA is formed early after rAAV-HBV infection at high levels but is lost over time. rAAV-HBV transduction of the mouse liver leads to long-lasting HBV viremia driven by the episomal AAV-HBV DNA without inducing robust immune response to rAAV vector resulting in its clearance. Thus, there is no doubt that rAAV-HBV mouse model is an invaluable tool to study HBV-specific immune tolerance and to evaluate novel antivirals or immunotherapeutic regimens directly targeting cccDNA molecules. Nonetheless, our data suggests a careful consideration of the rAAV-HBV mouse models for studying cccDNA biology as in this model cccDNA is established independent of HBV replication and rather short-lived.

Declaration of competing interest

The authors declare that they have no known competing financial interests or personal relationships that could have appeared to influence the work reported in this paper.

Acknowledgements

The work was funded by the German Research Foundation (DFG) via TRR179 (project No. 2378635) TP 14 and 18 (to UP) and by the German Center for Infection Research (DZIF, project TTU05.806). JS received a stipend from the Chinese Scholarship Council (CSC, File No.201504910672).

Appendix A. Supplementary data

Supplementary data to this article can be found online at <https://doi.org/10.1016/j.antiviral.2021.105140>.

References

Allweiss, L., Dandri, M., 2016. Experimental in vitro and in vivo models for the study of human hepatitis B virus infection. *J. Hepatol.* 64, S17–S31.

Bartenschlager, R., Junker-Niepmann, M., Schaller, H., 1990. The P gene product of hepatitis B virus is required as a structural component for genomic RNA encapsidation. *J. Virol.* 64, 5324–5332.

Boyd, A., Lacombe, K., Lavocat, F., Maylin, S., Miallhes, P., Lascoux-Combe, C., Delaugerre, C., Girard, P.M., Zoulim, F., 2016. Decay of ccc-DNA marks persistence of intrahepatic viral DNA synthesis under tenofovir in HIV-HBV co-infected patients. *J. Hepatol.* 65, 683–691.

Choi, V.W., McCarty, D.M., Samulski, R.J., 2006. Host cell DNA repair pathways in adeno-associated viral genome processing. *J. Virol.* 80, 10346–10356.

Davidoiff, A.M., Gray, J.T., Ng, C.Y., Zhang, Y., Zhou, J., Spence, Y., Bakar, Y., Nathwani, A.C., 2005. Comparison of the ability of adeno-associated viral vectors pseudotyped with serotype 2, 5, and 8 capsid proteins to mediate efficient transduction of the liver in murine and nonhuman primate models. *Mol. Ther.* 11, 875–888.

Dion, S., Bourguine, M., Godon, O., Levillayer, F., Michel, M.-L., 2013. Adeno-associated virus-mediated gene transfer leads to persistent hepatitis B virus replication in mice expressing HLA-A2 and HLA-DR1 molecules. *J. Virol.* 87, 5554–5563.

Dong, J.Y., Fan, P.D., Frizzell, R.A., 1996. Quantitative analysis of the packaging capacity of recombinant adeno-associated virus. *Hum. Gene Ther.* 7, 2101–2112.

Duan, D., Sharma, P., Yang, J., Yue, Y., Dudus, L., Zhang, Y., Fisher, K.J., Engelhardt, J. F., 1998. Circular intermediates of recombinant adeno-associated virus have defined structural characteristics responsible for long-term episomal persistence in muscle tissue. *J. Virol.* 72, 8568–8577.

Guidotti, L.G., Matzke, B., Schaller, H., Chisari, F.V., 1995. High-level hepatitis B virus replication in transgenic mice. *J. Virol.* 69, 6158–6169.

Hastie, E., Samulski, R.J., 2015. Adeno-associated virus at 50: a golden anniversary of discovery, research, and gene therapy success—a personal perspective. *Hum. Gene Ther.* 26, 257–265.

He, W., Ren, B., Mao, F., Jing, Z., Li, Y., Liu, Y., Peng, B., Yan, H., Qi, Y., Sun, Y., Guo, J. T., Sui, J., Wang, F., Li, W., 2015. Hepatitis D virus infection of mice expressing human sodium taurocholate Co-transporting polypeptide. *PLoS Pathog.* 11, e1004840.

Hirt, B., 1967. Selective extraction of polyoma DNA from infected mouse cell cultures. *J. Mol. Biol.* 26, 365–369.

Hu, J., Lin, Y.Y., Chen, P.J., Watashi, K., Wakita, T., 2019. Cell and animal models for studying hepatitis B virus infection and drug development. *Gastroenterology* 156, 338–354.

Kitamura, K., Que, L., Shimadu, M., Koura, M., Ishihara, Y., Wakae, K., Nakamura, T., Watashi, K., Wakita, T., Muramatsu, M., 2018. Flap endonuclease 1 is involved in cccDNA formation in the hepatitis B virus. *PLoS Pathog.* 14, e1007124.

Ko, C., Bester, R., Zhou, X., Xu, Z., Blossley, C., Sacherl, J., Vondran, F.W.R., Gao, L., Protzer, U., 2019. A new role for capsid assembly modulators to target mature hepatitis B virus capsids and prevent virus infection. *Antimicrob. Agents Chemother.* 64 e01440-1419.

Ko, C., Chakraborty, A., Chou, W.M., Hasreiter, J., Wettengel, J.M., Stadler, D., Bester, R., Asen, T., Zhang, K., Wisskirchen, K., McKeating, J.A., Ryu, W.S., Protzer, U., 2018. Hepatitis B virus genome recycling and de novo secondary infection events maintain stable cccDNA levels. *J. Hepatol.* 69, 1231–1241.

Ko, C., Shin, Y.C., Park, W.J., Kim, S., Kim, J., Ryu, W.S., 2014. Residues Arg703, Asp777, and Arg781 of the RNase H domain of hepatitis B virus polymerase are critical for viral DNA synthesis. *J. Virol.* 88, 154–163.

Koniger, C., Wingert, I., Marsmann, M., Rosler, C., Beck, J., Nassal, M., 2014. Involvement of the host DNA-repair enzyme TDP2 in formation of the covalently closed circular DNA persistence reservoir of hepatitis B viruses. *Proc. Natl. Acad. Sci. U. S. A.* 111, E4244–E4253.

Kosinska, A.D., Moeed, A., Kallin, N., Festag, J., Su, J., Steiger, K., Michel, M.L., Protzer, U., Knolle, P.A., 2019. Synergy of therapeutic heterologous prime-boost hepatitis B vaccination with CpG-application to improve immune control of persistent HBV infection. *Sci. Rep.* 9, 10808.

Lempp, F.A., Mutz, P., Lipps, C., Wirth, D., Bartenschlager, R., Urban, S., 2016a. Evidence that hepatitis B virus replication in mouse cells is limited by the lack of a host cell dependency factor. *J. Hepatol.* 64, 556–564.

Lempp, F.A., Qu, B., Wang, Y.X., Urban, S., 2016b. Hepatitis B virus infection of a mouse hepatic cell line reconstituted with human sodium taurocholate cotransporting polypeptide. *J. Virol.* 90, 4827–4831.

Li, H., Zhuang, Q., Wang, Y., Zhang, T., Zhao, J., Zhang, Y., Zhang, J., Lin, Y., Yuan, Q., Xia, N., Han, J., 2014. HBV life cycle is restricted in mouse hepatocytes expressing human NTCP. *Cell. Mol. Immunol.* 11, 175–183.

Long, Q., Yan, R., Hu, J., Cai, D., Mitra, B., Kim, E.S., Marchetti, A., Zhang, H., Wang, S., Liu, Y., Huang, A., Guo, H., 2017. The role of host DNA ligases in hepadnavirus covalently closed circular DNA formation. *PLoS Pathog.* 13, e1006784.

Lucifora, J., Salvetti, A., Marniquet, X., Mailly, L., Testoni, B., Fusil, F., Inchauspé, A., Michelet, M., Michel, M.L., Levrero, M., Cortez, P., Baumert, T.F., Cosset, F.L., Challier, C., Zoulim, F., Durantel, D., 2017. Detection of the hepatitis B virus (HBV) covalently-closed-circular DNA (cccDNA) in mice transduced with a recombinant AAV-HBV vector. *Antivir. Res.* 145, 14–19.

Luo, J., Cui, X., Gao, L., Hu, J., 2017. Identification of an intermediate in hepatitis B virus covalently closed circular (CCC) DNA formation and sensitive and selective CCC DNA detection. *J. Virol.* 91 e00539-517.

Michler, T., Kosinska, A.D., Festag, J., Bunse, T., Su, J., Ringelhan, M., Imhof, H., Grimm, D., Steiger, K., Mogler, C., Heikenwalder, M., Michel, M.L., Guzman, C.A., Milstein, S., Sepp-Lorenzino, L., Knolle, P., Protzer, U., 2020. Knockdown of virus antigen expression increases therapeutic vaccine efficacy in high-titer hepatitis B virus carrier mice. *Gastroenterology* 158, 1762–1775 e1769.

Nakai, H., Storm, T.A., Kay, M.A., 2000. Recruitment of single-stranded recombinant adeno-associated virus vector genomes and intermolecular recombination are responsible for stable transduction of liver in vivo. *J. Virol.* 74, 9451–9463.

Nassal, M., 2015. HBV cccDNA: viral persistence reservoir and key obstacle for a cure of chronic hepatitis B. *Gut* 64, 1972–1984.

Ni, Y., Lempp, F.A., Mehrle, S., Nkongolo, S., Kaufman, C., Falth, M., Stindt, J., Koniger, C., Nassal, M., Kubitz, R., Sultmann, H., Urban, S., 2014. Hepatitis B and D viruses exploit sodium taurocholate Co-transporting polypeptide for species-specific entry into hepatocytes. *Gastroenterology* 146, 1070–1083 e1076.

Nonnenmacher, M., Weber, T., 2012. Intracellular transport of recombinant adeno-associated virus vectors. *Gene Ther.* 19, 649–658.

Pillay, S., Meyer, N.L., Puschnik, A.S., Davulcu, O., Diep, J., Ishikawa, Y., Jae, L.T., Wosen, J.E., Nagamine, C.M., Chapman, M.S., Carette, J.E., 2016. An essential receptor for adeno-associated virus infection. *Nature* 530, 108–112.

Protzer, U., 2017. The bumpy road to animal models for HBV infection. *Nat. Rev. Gastroenterol. Hepatol.* 14, 327–328.

Qi, Y., Gao, Z., Xu, G., Peng, B., Liu, C., Yan, H., Yao, Q., Sun, G., Liu, Y., Tang, D., Song, Z., He, W., Sun, Y., Guo, J.T., Li, W., 2016. DNA polymerase kappa is a key cellular factor for the formation of covalently closed circular DNA of hepatitis B virus. *PLoS Pathog.* 12, e1005893.

Seeger, C., Mason, W.S., 2015. Molecular biology of hepatitis B virus infection. *Virology* 479–480C, 672–686.

Sheraz, M., Cheng, J., Tang, L., Chang, J., Guo, J.-T., 2019. Cellular DNA topoisomerases are required for the synthesis of hepatitis B virus covalently closed circular DNA. *J. Virol.* 93 e02230-2218.

Sprinzl, M.F., Oberwinkler, H., Schaller, H., Protzer, U., 2001. Transfer of hepatitis B virus genome by adenovirus vectors into cultured cells and mice: crossing the species barrier. *J. Virol.* 75, 5108–5118.

Tavis, J.E., Perri, S., Ganem, D., 1994. Hepadnavirus reverse transcription initiates within the stem-loop of the RNA packaging signal and employs a novel strand transfer. *J. Virol.* 68, 3536–3543.

Thomas, C.E., Storm, T.A., Huang, Z., Kay, M.A., 2004. Rapid uncoating of vector genomes is the key to efficient liver transduction with pseudotyped adeno-associated Virus Vectors. *J. Virol.* 78, 3110–3122.

Velkov, S., Ott, J.J., Protzer, U., Michler, T., 2018. The global hepatitis B virus genotype distribution approximated from available genotyping data. *Genes* 9, 495.

Wang, L., Cao, M., Wei, Q.L., Zhao, Z.H., Xiang, Q., Wang, H.J., Zhang, H.T., Lai, G.Q., 2017. A new model mimicking persistent HBV e antigen-negative infection using covalently closed circular DNA in immunocompetent mice, 12, e0175992.

Wei, L., Ploss, A., 2020. Core components of DNA lagging strand synthesis machinery are essential for hepatitis B virus cccDNA formation, 5, 715–726.

WHO, 2019. Hepatitis B, Fact Sheet.

- Wu, M., Wang, C., Shi, B., Fang, Z., Qin, B., Zhou, X., Zhang, X., Yuan, Z., 2020. A novel recombinant cccDNA-based mouse model with long term maintenance of rcccDNA and antigenemia. *Antivir. Res.* 180, 104826.
- Yan, H., Peng, B., He, W., Zhong, G., Qi, Y., Ren, B., Gao, Z., Jing, Z., Song, M., Xu, G., Sui, J., Li, W., 2013. Molecular determinants of hepatitis B and D virus entry restriction in mouse sodium taurocholate cotransporting polypeptide. *J. Virol.* 87, 7977–7991.
- Yan, H., Zhong, G., Xu, G., He, W., Jing, Z., Gao, Z., Huang, Y., Qi, Y., Peng, B., Wang, H., Fu, L., Song, M., Chen, P., Gao, W., Ren, B., Sun, Y., Cai, T., Feng, X., Sui, J., Li, W., 2012. Sodium taurocholate cotransporting polypeptide is a functional receptor for human hepatitis B and D virus. *eLife* 1, e00049.
- Yan, Z., Zeng, J., Yu, Y., Xiang, K., Hu, H., Zhou, X., Gu, L., Wang, L., Zhao, J., Young, J. A.T., Gao, L., 2017. HBVcircle: a novel tool to investigate hepatitis B virus covalently closed circular DNA. *J. Hepatol.* 66, 1149–1157.
- Yang, D., Liu, L., Zhu, D., Peng, H., Su, L., Fu, Y.-X., Zhang, L., 2014. A mouse model for HBV immunotolerance and immunotherapy. *Cell. Mol. Immunol.* 11, 71–78.